Numerical Finger Kinematic Models Derived From Virtual Grasping of Various Cylindrical Objects With the Family of Conic Sections

Jong-Seob Won
Department of Mechanical and Automotive Engineering,
Jeonju University,
Jeonju-si, Jullabuk-do 55069, South Korea
e-mail: jswon@jj.ac.kr

Reza Langari
Department of Mechanical Engineering,
Texas A&M University,
College Station, TX 77840
e-mail: rlangari@tamu.edu

Nina Robson[1]
Department of Mechanical Engineering,
California State University,
Fullerton, CA 92834
e-mail: nrobson@fullerton.edu

In this study, a numerical framework for joint rotation configuration models of a finger is proposed. The basic idea is to replicate the finger's geometric posture observed when the human hand grasps a cylindrical object with various cross sections. In the model development, objects with the cross section adopted from the curves of order two (the family of conic sections) are taken into consideration to realize various finger postures. In addition, four different grasp styles, which simulate the individual-specific contact pattern between the surfaces of object and finger, are modeled and applied for the formulation of numerical models. An idea on how to change flexion/extension patterns in the middle of excursion of movement is proposed and discussed. Series of numerical studies have been conducted and analyzed to evaluate the proposed models. From the results, one can see the models' feasibility and viability as a solution to describing finger's flexion/extension movements (FEMs) for grasping patterns.
[DOI: 10.1115/1.4048257]

Keywords: finger kinematic model, numerical approach, conic section, grasping style, object manipulation

1 Introduction

There have been many needs on simulating flexion and/or extension of fingers in various areas of applications—medicine and rehabilitation, prosthetics, artificial hands, robotics, man–machine interface device, human–computer interaction, and so on. Following the needs, a numerous research have been conducted in regard to human fingers simulation [1], finger motion coordination [2–4], virtual hand modeling and simulation [5–9], and articulated human hand [10,11].

In the model development, the following two aspects should be taken into consideration to fully describe flexion/extension functions of a finger: (1) joint rotation configuration in the viewpoint of inter-joint coordination and (2) the pattern with which a finger moves during the excursion of flexion/extension movement. Joint rotation configuration is related to the calculation of joint rotation angles in the stage of finger motion. The pattern is related to the mode of behavior of the finger during the flexion and/or extension.

In our recent work [9], the authors proposed a geometric approach to the development of a finger kinematic model for joint rotation configuration. Based on the finger posture observed when the hand grasps round-shaped cylinders, the geometric relations between the finger and the object are taken into consideration and the formula for joint rotation angle calculation is derived for each joint. The advantage of the model is that it provides three independent formulas for calculating the rotational angle of each joint, and only one parameter is involved for determining joint rotation configuration of a finger during flexion and/or extension. This allows the model to be utilized to robotic finger/hand control system design for multi-finger coordination. It is noted from motion capture experiments that the proposed model can simulate a naturalistic behavior of an index finger of the human hand as closely as possible.

On the basis of the recent research, the authors propose a numerical framework for joint position configuration of a finger by diversifying the shape of the virtual object being grasped and the way by which a finger encompasses the object. The model proposed in the preceding paper [9] deemed adequate to describe a grasping motion with a full fist, yet showed some inadequacy to describe a pinching motion that required in fine robot hand manipulation. While the grasping motion, a good fundamental of a robot hand manipulation, a robot requires a pinching motion as well. Such an alternative grasping motion allows a fine manipulation that complements the large workspace that a conventional grasping motion possesses and further allows better-grasping capability for elongated objects such as books. The proposed model describes well of the listed motion, while it shares the same manipulation method as the proposed motion from the previous research.

In the present work, the authors consider various virtual objects with different shapes of cross sections taken from curves of order two (conic sections)—circle, ellipse, parabola, and hyperbola. The equation of each curve is involved as one geometric condition in the numerical model. The fundamental of complex gesture of the hand resides in grasping motion in circular "frame" for many of the shapes can be inscribed in a circle. To tightly grasp the object being manipulated, the proposed method with different contact patterns can be applied. Thus, a cylindrical assumption lays the groundwork for further manipulation. During the grasping motion, each phalanx may abduct or adduct to their needs. If the object of interest can be hypothesized to be a cylindrical object, a cross section that denoted by an operational plane, formed by points of metacarpophalangeal (MCP), proximal interphalangeal (PIP), and distal interphalangeal (DIP), forms one of the listed shapes, i.e., a circle, an ellipse, a parabola, and a hyperbola. Thus, each finger can be coordinated to its corresponding cross section. Another consideration in the development of the model is to formularize the way the hand and object come into contact. Four different contact types (referred to as a grasp style, hereafter) are modeled and investigated.

It is noted that although the advantages and their modeling directions of the previous researches are best explained, this work focuses on the expansion of our previous work and the establishment of geometry-based numerical finger kinematic models. This article is organized as follows. In Sec. 2, a numerical framework for geometry-based finger kinematic models that can determine the joint angle configuration of the index finger is proposed. By introducing various virtual objects with different cross sections taken from curves of order two and grasp styles, numerical models corresponding to objects each by contact methods are developed. In Sec. 3, the results from numerical simulation studies are discussed. Section 4 proposes a method to deal with a flexion/extension pattern transition during the excursion of the finger movement. Finally, Sec. 5 concludes this paper with the summary of the work.

[1]Corresponding author.

Contributed by the Mechanisms and Robotics Committee of ASME for publication in the Journal of Mechanisms and Robotics. Manuscript received October 21, 2019; final manuscript received August 11, 2020; published online October 7, 2020. Assoc. Editor: Gim Song Soh.

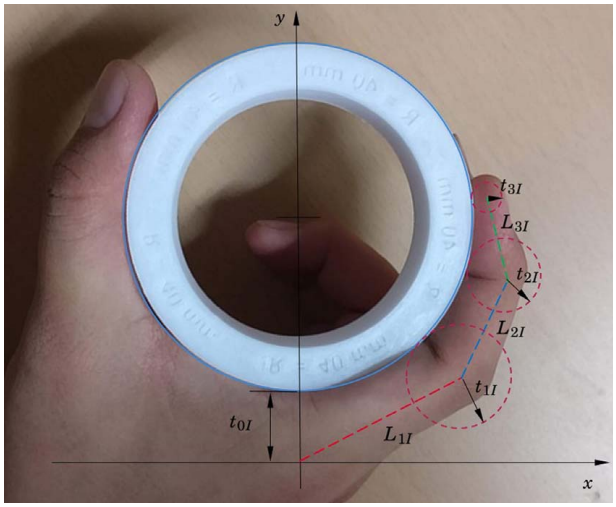

Fig. 1 Finger posture in the geometric viewpoint. Notes: The dotted lines represent proximal, middle, and distal phalangers, respectively. The origin is on the MCP joint. L_{il}, length of phalanx i, t_{il}, distance from the surface to the skeleton corresponding to each joints and the fingertip.

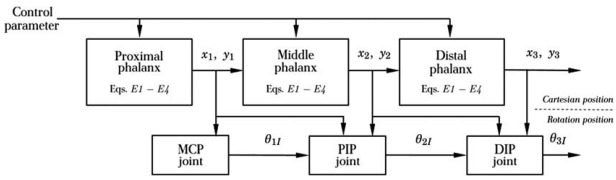

Fig. 2 Numerical framework for calculating the joint angles of a finger (modified from Ref. [9])

2 Numerical Framework for Joint Angle Configuration Models

2.1 Numerical Model Structure. The notion adopted to develop joint angle configuration models is based on the geometric finger posture, which may be observed when an index finger softly encompasses the surface of a virtual cylindrical object (see Fig. 1). For the models development on the basis of the notion mentioned earlier, the authors adopted the structure of joint angle calculation process introduced in our previous work [9], as shown in Fig. 2.

In the Cartesian position part, there are three blocks each of which is corresponding to the *i*th phalanx and provides its Cartesian position. Each block consists of four equations: equation *E1* is related to the shape of virtual object being grasped—an equation of cross section; equations *E2* and *E3* are to the geometry of phalanx—length of phalanx and thickness of joint (i.e., distance from surface to skeleton), respectively; equation *E4* is to grasp style by which the finger encompasses an object.

The joint angles of a finger can be obtained in the Rotation position part via trigonometric formulas with the Cartesian position provided.

2.2 Virtual Objects With Conic Sections. To have finger kinematic models for the joint angle configuration, the authors deal with cylindrical objects with the cross section constructed by a conic section (or *conic*).

A conic section is obtained from the intersection of a right circular cone with a plane. There are four types of conic sections: circle, ellipse, parabola, and hyperbola.

The information about the family of conic sections for a right circular cone is summarized in Table 1 [12].

Five types of right cylindrical objects with different cross sections are considered in deriving geometric finger kinematic models for the joint angle configuration: cylinder, cylindroid, parabolic cylinder, hyperbolic cylinder, and triangular prism. It is noted that the triangular prism is also taken into consideration, since its cross section can be constructed from the asymptote of a hyperbola.

Table 1 Conic sections with its characteristic features

	Circle	Ellipse	Parabola	Hyperbola
	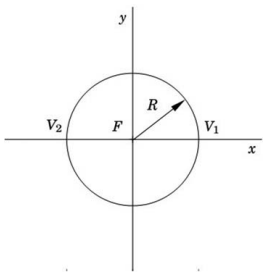	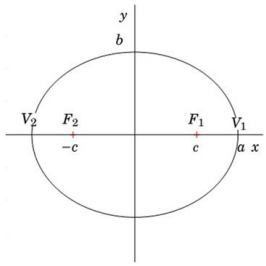	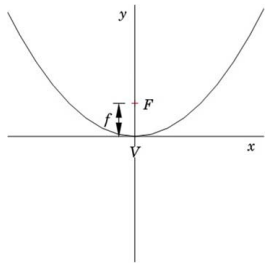	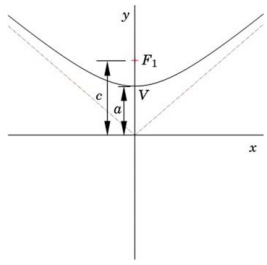
Eq.	$\frac{x^2}{R^2}+\frac{y^2}{R^2}=1$	$\frac{x^2}{a^2}+\frac{y^2}{b^2}=1$	$y=\frac{1}{4f}x^2$	$\frac{x^2}{b^2}-\frac{y^2}{a^2}=-1$
d	0	c	f	c
l	∞	$\frac{a^2}{c}$	$-f$	$\frac{c^2}{a}$
e	0	$\frac{c}{a}$	1	$\frac{c}{a}$
p	R	$\frac{b^2}{a}$	$2f$	$\frac{b^2}{a}$
CP	R	a, c	f	a, c
Remarks	–	$b^2=a^2-c^2$	–	$b^2=c^2-a^2$

Note: F_i, focus; V_i, vertex; d, focal distance; l, directrix; e, numerical eccentricity; p, semi-latus rectum; CP, shape parameter.

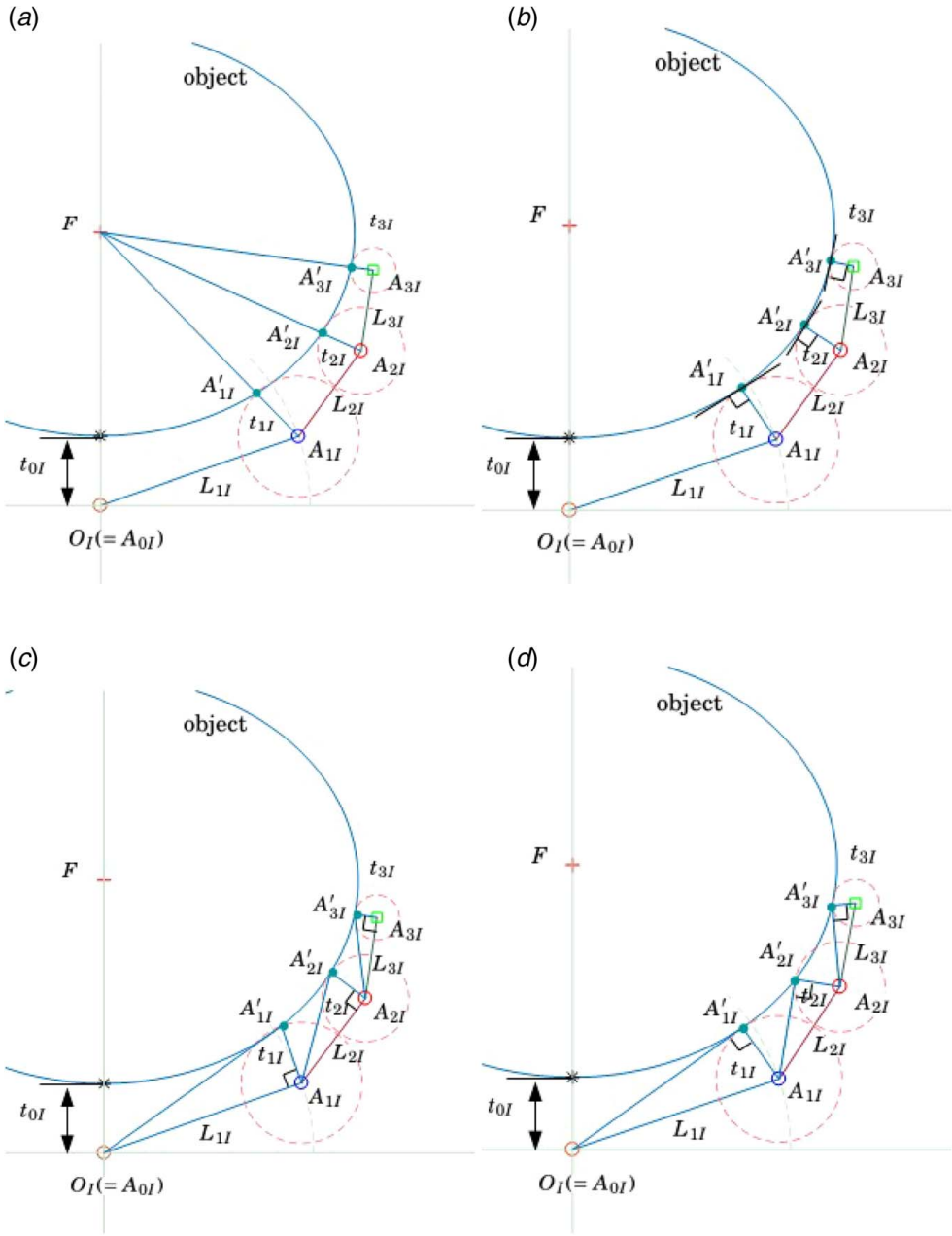

Fig. 3 Grasp style modeling for joint rotation configuration models development: (*a*) method 0 (M0), (*b*) method 1 (M1), (*c*) method 2 (M2), and (*d*) method 3 (M3)

2.3 Grasp Style Modeling. In the model development, four different grasp styles are modeled and introduced to consider diversity of individual-specific flexion movements as shown in Fig. 3.

Joint angle configuration models are used to provide the joint angles of a finger during flexion and/or extension movement. In the model point of view, the angles are calculated by the Cartesian positions of phalangers.

Along grasp styles, the way with which an object and fingers come into contact is varied in determining the position of each joint.

Table 2 Relationship between lines in each grasp style

M0	M1	M2	M3
$l_{F2Ii} \parallel l_{Ii}$	$l_{Ti} \perp l_{Ii}$	$l_{Pi} \perp l_{Ii}$	$l_{J2Ii} \perp l_{Ii}$

Table 3 Systems of nonlinear equations per each grasp style for grasping simulation with circular cross section for joint angle calculation of phalanx *i*

Eq.	M0 $l_{F2Ii} \parallel l_{Ii}$	M1 $l_{Ti} \perp l_{Ii}$	M2 $l_{Pi} \perp l_{Ii}$	M3 $l_{J2Ii} \perp l_{Ii}$
E1	$\frac{x_i'^2}{R^2} + \frac{(y_i' - (R + t_{0I}))^2}{R^2} = 1$	←[a]	←	←
E2	$(x_i - x_{i-1})^2 + (y_i - y_{i-1})^2 = L_{iI}^2$	←	←	←
E3	$(x_i - x_i')^2 + (y_i - y_i')^2 = t_{iI}^2$	←	←	←
E4	$s_{F2Ii} = s_{Ii}$	$s_{Ti} \cdot s_{Ii} = -1$	$s_{Pi} \cdot s_{Ii} = -1$	$s_{J2Ii} \cdot s_{Ii} = -1$

Note: $s_{F2Ii} = \frac{y_i' - (R + t_{0I})}{x_i'}$, $s_{Ti} = -\frac{x_i'}{y_i' - (R + t_{0I})}$, $s_{Ii} = \frac{y_i - y_i'}{x_i - x_i'}$, $s_{Pi} = \frac{y_i - y_{i-1}}{x_i - x_{i-1}}$, $s_{J2Ii} = \frac{y_i' - y_{i-1}}{x_i' - x_{i-1}}$.

[a] ←: same as left.

Table 4 Equation representing a conic section and definition of object (conic)-dependent slopes (s_{F2Ii} and s_{Ti}) incorporated in system of nonlinear equations

Conic	E1	s_{F2Ii}	s_{Ti}
Circle	$\frac{x_i'^2}{R^2}+\frac{(y_i'-(R+t_{0I}))^2}{R^2}=1$	$\frac{y_i'-(R+t_{0I})}{x_i'}$	$-\frac{x_i'}{y_i'-(R+t_{0I})}$
Ellipse	$\frac{x_i'^2}{a^2}+\frac{(y_i'-(b+t_{0I}))^2}{b^2}=1$	$\frac{y_i'-(b+t_{0I})}{x_i'}$	$-\left(\frac{b^2}{a^2}\right)\frac{x_i'}{y_i'-(b+t_{0I})}$
Parabola	$y_i'=\frac{1}{4f}x_i'^2+t_{0I}$	$\frac{y_i'-(f+t_{0I})}{x_i'}$	$\frac{1}{2f}x_i'$
Hyperbola	$\frac{x_i'^2}{b^2}-\frac{(y_i'-c)^2}{a^2}=-1$	$\frac{y_i'-c}{x_i'}$	$\frac{a^2}{b^2}\frac{x_i'}{y_i'}$
Triangle	$y_i'=\frac{a}{b}x_i'$	$\frac{y_i'-c}{x_i'}$	$\frac{y_i-y_i'}{x_i-x_i'}$

Table 5 Control (shape) parameter of respective cross sections, which governs flexion/extension motions of finger models

	Conic section				
	Circle	Ellipse	Parabola	Hyperbola	Asymptote
Control parameter	R	a (for fixed $e \to b$)	f	c (for $a=t_{0I} \to b$)	← ←

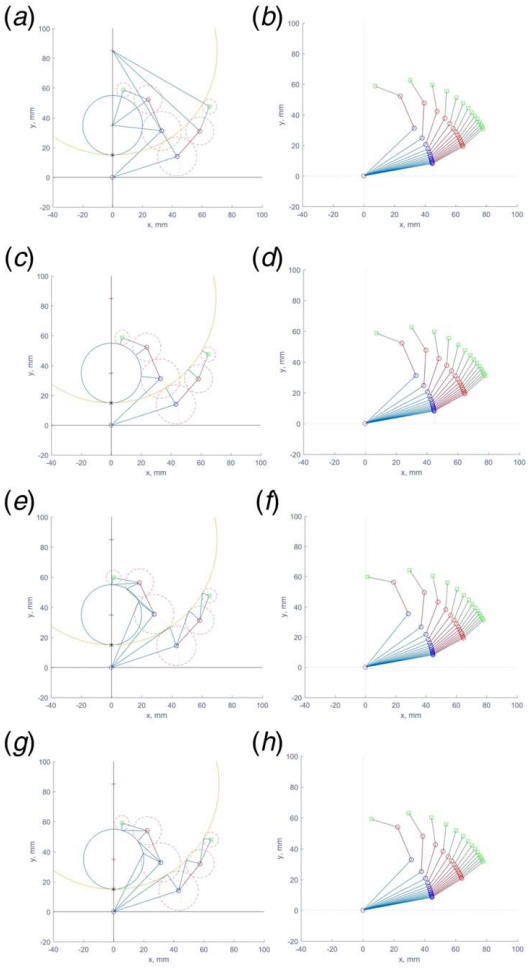

Fig. 4 Numerical simulation example for an object with a circular cross section. Notes: First column, an example of the finger motion for each corresponding contact method; second column, the simulated stepwise motion of finger joints (displayed for different values of the control parameter associated with the conic section under consideration).

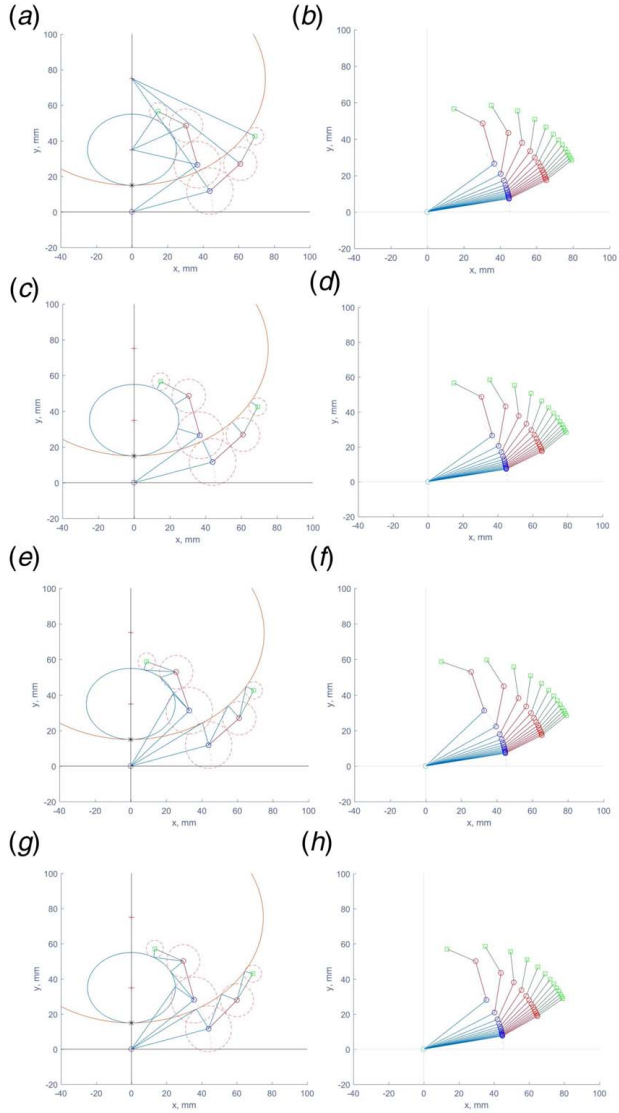

Fig. 5 Numerical simulation example for an object with an elliptic cross section ($a > b$). Notes: First column, an example of the finger motion for each corresponding contact method; second column, the simulated stepwise motion of finger joints (displayed for different values of the control parameter associated with the conic section under consideration).

These styles can be characterized by the "slope condition" among lines defined on the object and phalangers.

Before proceeding, a basic notation is given first. F is the focus (or center) of a conic section. A_{iI}', (x_i', y_i') is the intersection point on the conic corresponding to the point A_{iI}, (x_i, y_i) on the phalanx i. A_{0I}, A_{1I}, and A_{2I} are the points attached to MCP, PIP, and DIP joints, respectively. A_{3I} represents the fingertip.

Based on the notation earlier, the following lines (or line segments) are defined: $l_{F2Ii}=\overline{FA_{iI}'}$, $l_{iI}=\overline{A_{iI}'A_{iI}}$, l_{Ti} is the tangent line on A_{iI}', l_{Pi} is a line in parallel with the phalanx i and $l_{J2Ii}=\overline{A_{iI}'A_{(i-1)I}}$. Subscript I represents the index finger.

With the lines (or line segments) defined earlier, the grasp styles shown in Fig. 3 can be described by the relationship among lines (referred to as "slope condition," hereafter) shown in Table 2. Note that in grasp style models M0 and M1, lines defined on the object being grasped are mainly taken into consideration (i.e., related to the object shape); on the other hand, M2 and M3 feature lines defined outside of the object (i.e., related to the finger shape). Furthermore, it is noted that the method M0 is introduced in our previous work [9].

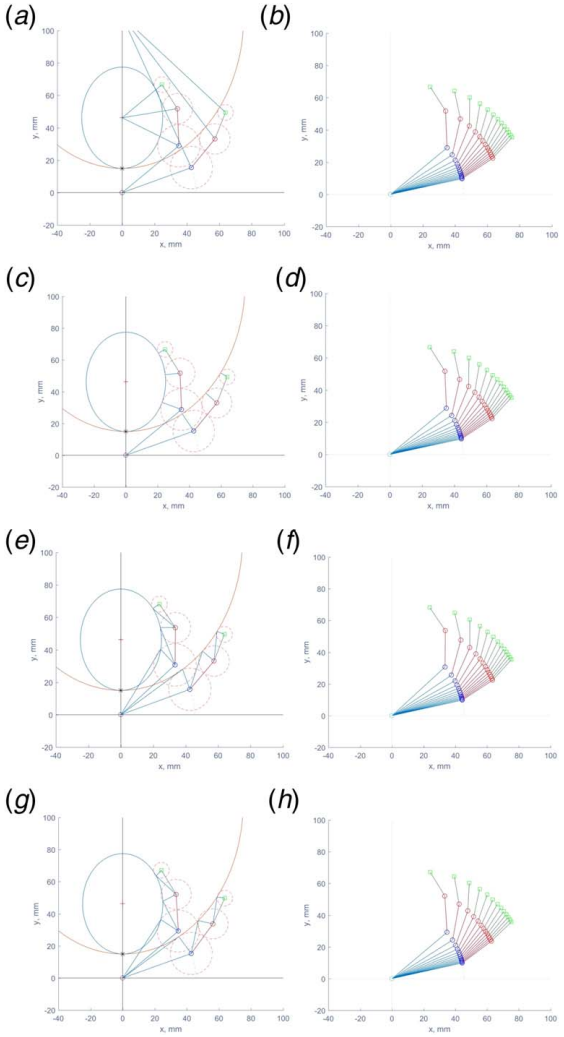

Fig. 6 Numerical simulation example for an object with an elliptic cross section ($a < b$). Notes: First column, an example of the finger motion for each corresponding contact method; second column, the simulated stepwise motion of finger joints (displayed for different values of the control parameter associated with the conic section under consideration).

2.4 Systems of Nonlinear Equations for Numerical Simulation. For joint angle calculation of the finger grasping an object with a circular cross section, Table 3 lists the system of nonlinear equations for joint angle calculation of phalanx i, which incorporates grasp styles adopted each. The explanation on each equation *E1* – *E4* is given in Sec. 2.1. The slope condition in Table 2 of each grasp style modeling can be formulated by slopes of lines defined in Sec. 2.3. The slopes of lines defined here are given in Table 3.

For objects with various cross sections, *E1* and the object (cross section)-dependent slopes s_{F2Ii} and s_{Ti} (encompassed in the solid box) in Table 3 can be replaced with ones in Table 4. Note that the slopes s_{F2Ii} and s_{Ti} are calculated by the lines defined on the object at hand.

To achieve a joint angle configuration of a finger via systems of equations in Tables 3 and 4, one needs to rely on numerical methods to obtain solutions of the equations due to their nonlinear features. Figure 2 shows how the joint angle of each joint of MCP, PIP, and DIP, respectively, is calculated in the consecutive order. It is worth to note that the model has one degree-of-freedom that is capable of describing the joint rotation configuration of an index finger (with three degrees of rotation freedom) by a single shape parameter listed in Table 5. The shape parameter can be called the control parameter since the shape parameter can be used to change its shape of the cross section in the control point of view.

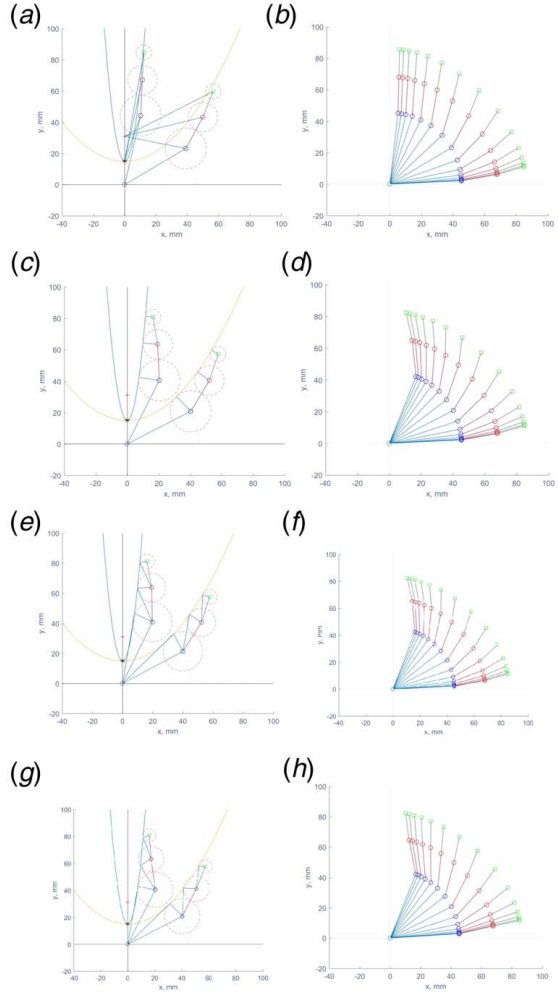

Fig. 7 Numerical simulation example for an object with a parabolic cross section. Notes: First column, an example of the finger motion for each corresponding contact method; second column, the simulated stepwise motion of finger joints (displayed for different values of the control parameter associated with the conic section under consideration).

3 Numerical Simulation Results

By using systems of nonlinear equations presented in Tables 3 and 4, numerical simulations have been carried out to see the behavior of the finger movement under a virtual grasping of the cylindrical object with a specific cross section. The control parameter listed in Table 5 was used to control the shape of each cross section. Four different grasp type models are adopted for objects each during the numerical simulation study. Simulations have been run following the joint angle calculation process as shown in Fig. 2.

The following anthropometric values of the semi-thickness and phalanx's length of the index finger under consideration are used for simulation: $t_{0I} = 1.5$, $t_{1I} = 1.31$, $t_{2I} = 0.94$, $t_{3I} = 0.49$, $L_1 = 4.54$, $L_2 = 2.29$, and $L_3 = 1.76$ (unit, cm). These values were taken from a specific subject participated in this study.

Figures 4–9 depicts the simulated motion derived by solving the equations. Plots on the left side exemplify the finger motion of each corresponding grasp style, whereas the right side illustrates the continuous stepwise posture for each of four grasp styles. Figure 10 provides fingertip trajectory comparison by methods for respective

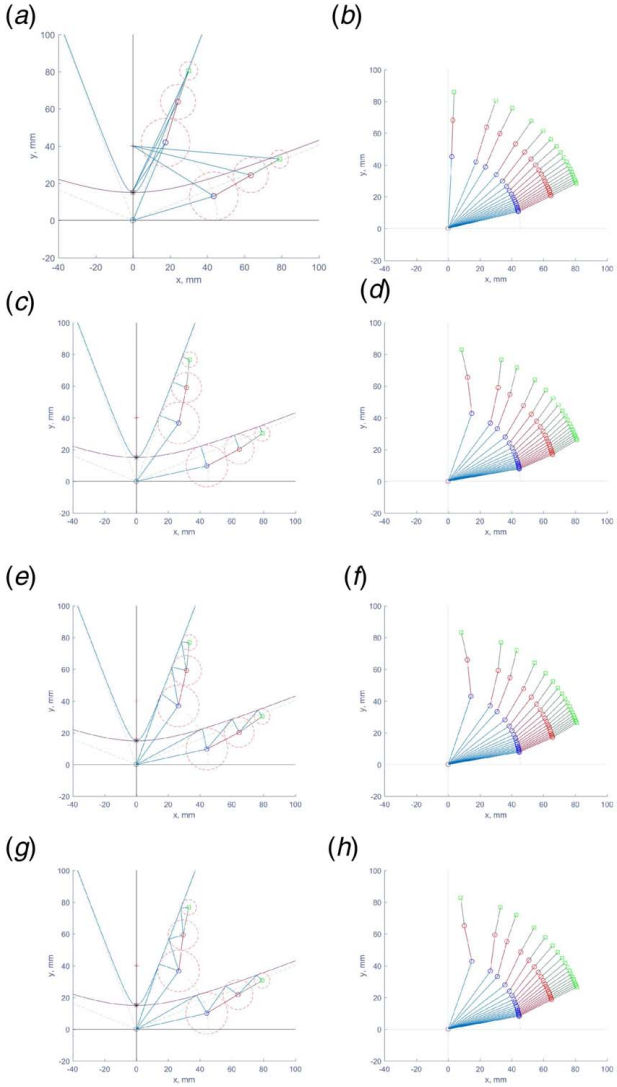

Fig. 8 Numerical simulation example for an object with a hyperbolic cross section. Notes: First column, an example of the finger motion for each corresponding contact method; second column, the simulated stepwise motion of finger joints (displayed for different values of the control parameter associated with the conic section under consideration).

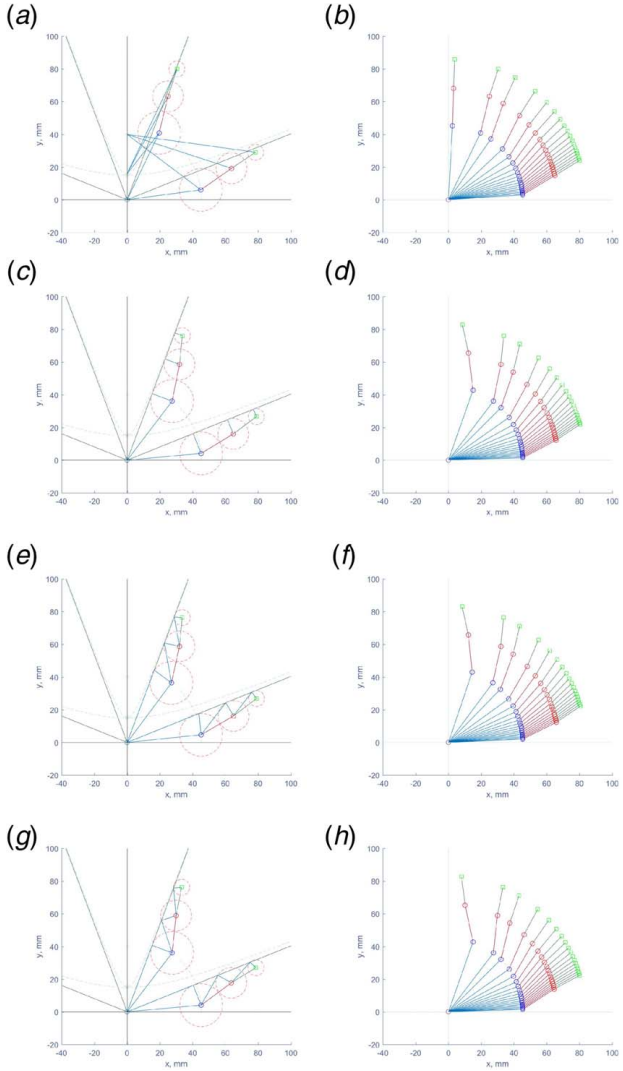

Fig. 9 Numerical simulation example for an object with a triangular cross section (from asymptote of hyperbola). Notes: First column, an example of the finger motion for each corresponding contact method; second column, the simulated stepwise motion of finger joints (displayed for different values of the control parameter associated with the conic section under consideration).

object of different cross sections. The following notion can be drawn from the observation of simulation results:

(1) The selection of a specific contact method can be made depending on the shape of object being grasped. It means that it needs not to apply an identical method to all objects with different cross sections.
(2) For objects with round-shaped cross sections, such as circles and ellipses, the choice of method M0 is preferred in the viewpoint of geometrical naturalness in posture.
(3) For objects with cross sections of a general curve (shape), there may be a limitation to the use of method M1, since it is not trivial to get the tangent formula of the curve.
(4) For objects with a small size, methods M2 and/or M3 cannot be applied since there are cases of "no-contact" between object and finger.
(5) As long as fingertip trajectory comparison, the locus of fingertip calculated by method M2 (M0) is large in closed (open)-curve cross sections.

4 Flexion/Extension Movement Pattern and Its Transition

The basic motion in fingers include flexion and extension. Grasping motion can be realized through a series of finger motions along with different degrees of flexion and/or extension. In the previous sections, joint angle configuration models for realizing FEM of a finger have been derived by assuming that fingers encompass a cylindrical object with the cross section taken from the family of conic sections. In this section, the authors investigate a method to deal with a FEM pattern change during the excursion of finger movement. Here, the FEM pattern can be defined as one that is observed during the behavior of grasping a cylindrical object with a specific cross section. Six patterns are discussed in this study (see Figs. 4–9).

The main notion of the FEM pattern change is based on the following scenario. During a flexion/extension motion of a finger with a given FEM pattern, one needs to change the current FEM pattern with another for performing specific grasping tasks. The basic idea proposed here is to use the semi-latus rectum p, which is one of the common characteristic features of the conic sections. Latus rectum

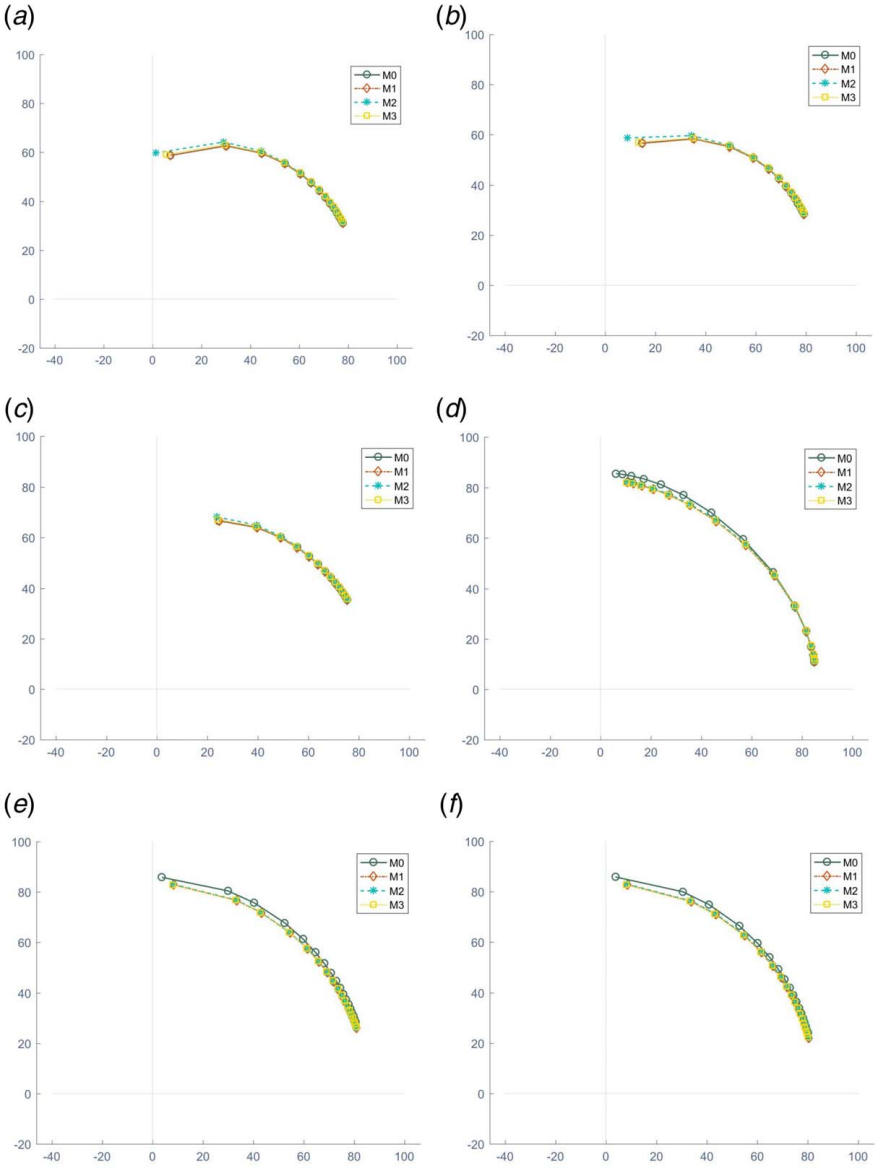

Fig. 10 Fingertip trajectory comparison by methods: (*a*) circle, (*b*) ellipse ($a > b$), (c) ellipse ($a < b$), (*d*) parabola, (e) hyperbola, and (*f*) triangle

is a chord perpendicular to the axis of the conic section through the focus and whose end pairs lie on the conic section (refer to Table 1). Figure 11 shows the different conic sections with the same value of p. This value is used as a reference to the starting posture of the new pattern, which will be discussed later.

Before proceeding, a twofold structure $S(\mathcal{T}, \mathcal{CP}(t))$ is introduced to make the description of FEM pattern changes simple. $S(\mathcal{T}, \mathcal{CP}(t))$ is a mathematical construct that represents the equation of a conic section. This consists of two parts: (1) $\mathcal{T} \in \{C, E^a, E^b, P, H, T\}$ is the type of cross section of the object being grasped and (2) $\mathcal{CP}(t)$ is the shape parameter of a cross section $\mathcal{T}$ and is controlled over time during flexion/extension movements. The capital letters C, E, P, H, and T represent a circle, an ellipse, a parabola, a hyperbola, and a triangle, respectively.

Let us start discussions with Fig. 12. Also, let us assume that a finger moves under the FEM pattern represented by $\mathcal{T}^-$. The coordinates of joints in the finger can be obtained by solving systems of nonlinear equations including $\mathcal{S}(\mathcal{T}^-, \mathcal{CP}(t))$. When the demands for FEM pattern change comes in, semi-latus rectum p of a circle is calculated for the use in setting the starting posture of finger with the new pattern $\mathcal{T}^+$ at time $t = t_t$. The superscript "-" and "+" in $\mathcal{T}$

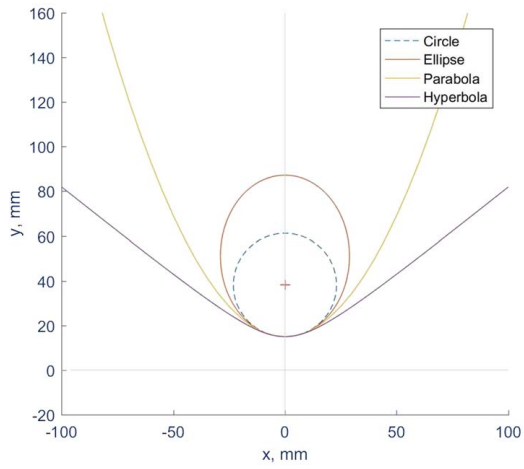

Fig. 11 Example of conic sections with the same latus rectum ($p = 23.1194$ mm). Notes: numerical eccentricity of ellipse, $e = 0.6$ and numerical eccentricity of hyperbola, $e = 1.5946$.

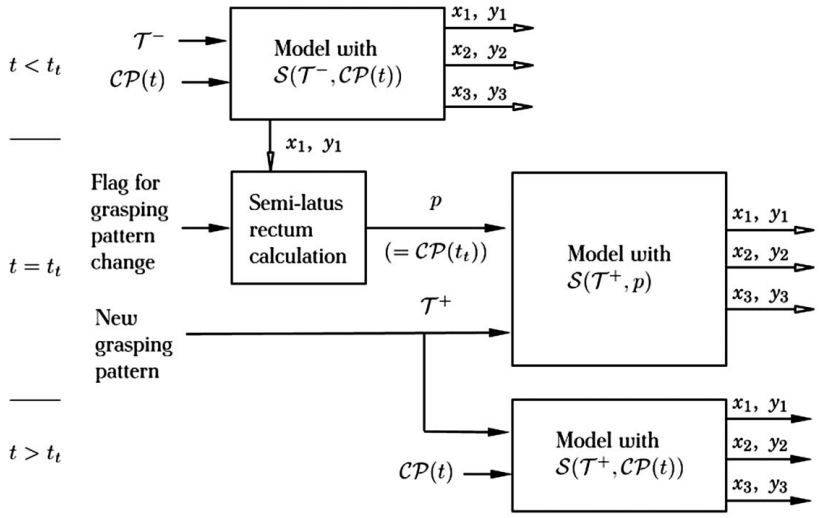

Fig. 12 Pattern change process

Table 6 Equation for cross section along with shape parameters for the application to pattern change

	Equation $\mathcal{S}(\mathcal{T}, \mathcal{CP}(t))$	Shape parameter in $\mathcal{S}(\mathcal{T}, \mathcal{CP}(t))$ at $t = t_t$	Shape parameter in $\mathcal{S}(\mathcal{T}, \mathcal{CP}(t))$ at $t > t_t$
Circle $\mathcal{T} = C$	$\frac{x'^2}{R(t)^2} + \frac{(y' - (R(t) + t_{0I}))^2}{R(t)^2} = 1$	$\mathcal{CP} = p$, $p = R$ (given) $R(t) = p$	$\mathcal{CP} = R(t)$
Ellipse $\mathcal{T} = E^a$	$\frac{x'^2}{a(t)^2} + \frac{(y' - (b(t) + t_{0I}))^2}{b(t)^2} = 1$	$\mathcal{CP} = p$, $p = R$ (given), for fixed e, $a(t) = \frac{p}{1 - e^2}$, $b(t) = \frac{p}{\sqrt{1 - e^2}}$ $(a > b)$	$\mathcal{CP} = a(t)$, for fixed e, $b(t) = a(t)\sqrt{1 - e^2}$ $(a > b)$
$\mathcal{T} = E^b$		$a(t) = \frac{p}{\sqrt{1 - e^2}}$, $b(t) = \frac{p}{1 - e^2}$ $(a < b)$	$b(t) = a(t)/\sqrt{1 - e^2}$ $(a < b)$
Parabola $\mathcal{T} = P$	$y' = \frac{1}{4f(t)}x'^2 + t_{0I}$	$\mathcal{CP} = p$, $p = R$ (given) $f(t) = \frac{p}{2}$	$\mathcal{CP} = f(t)$
Hyperbola $\mathcal{T} = H$	$\frac{x'^2}{b(t)^2} - \frac{(y' - c(t))^2}{a(t)^2} = -1$	$\mathcal{CP} = p$, $p = R$ (given) $a(t) = t_{0I}$: fixed $b(t) = \sqrt{p \cdot a(t)}$ $c(t) = \sqrt{a(t)^2 + b(t)^2}$	$\mathcal{CP} = c(t)$ $a(t) = t_{0I}$: fixed $b(t) = \sqrt{c(t)^2 - a(t)^2}$
Triangle $\mathcal{T} = T$	$y' = \frac{a(t)}{b(t)}x'$	↑	↑

Note: e is the numerical eccentricity.

represent before and after pattern transitions, respectively. The semi-latus rectum p of a circle is equal to the radius R of the circle and is obtained by the following formula (from Ref. [9]) with $\theta_1 = atan2(y_1, x_1)$, where (x_1, y_1) is the coordinates of the PIP joint of the finger at the time immediately before the demands comes in.

$$R(t_t) = -\frac{1}{2}\frac{t_{0I}^2 - 2t_{0I}L_{1I} + L_{1I}^2 - t_{1I}^2 + 4\left(\cos\left(1/4\,\pi + 1/2\,\theta_1\right)\right)^2 L_{1I}t_{0I}}{t_{0I} - L_{1I} - t_{1I} + 2\left(\cos\left(1/4\,\pi + 1/2\,\theta_1\right)\right)^2 L_{1I}} \tag{1}$$

Independent to previous formation (i.e., pattern), a transformation is made from utilizing the identical p value that achieved from Eq. (1). At $t = t_t$, the coordinates of each joint in the finger is obtained by solving the systems of nonlinear equations including $\mathcal{S}(\mathcal{T}^+, p)$. This is the starting posture of the finger with the newly changed pattern. After $t > t_t$, flexion and/or extension are performed under the newly changed pattern defined by $\mathcal{S}(\mathcal{T}^+, \mathcal{CP}(t))$ with the profile of shape parameter $\mathcal{CP}(t)$. Table 6 lists equations of cross sections with the shape parameter utilized during the pattern change. Figure 13 shows two examples of pattern change. Depending on the preceding pattern, the transition of finger posture can be either forward or backward at the time of transition. It is because that the succeeding patterns are defined with the semi-latus rectum obtained from the preceding pattern during the pattern change. It is worth to note that during pattern

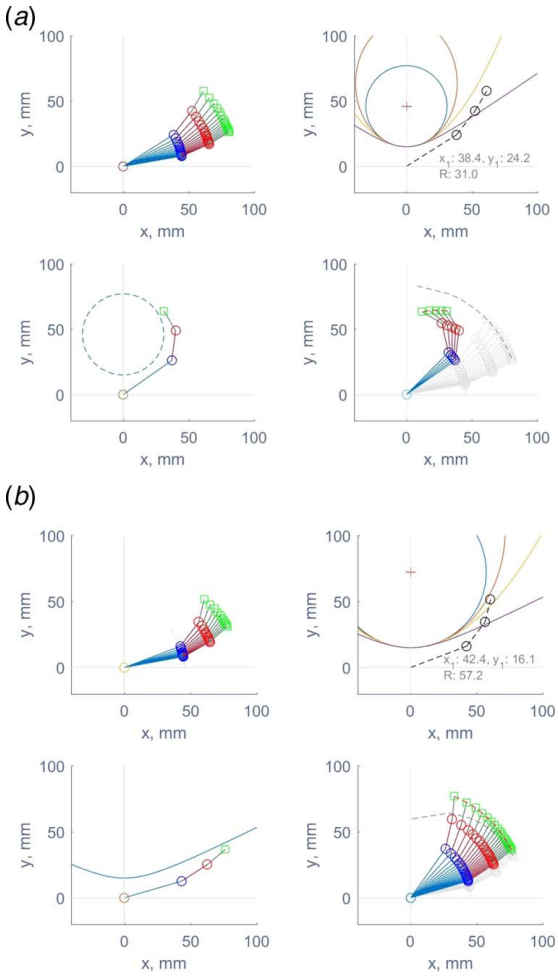

Fig. 13 Examples of pattern transition: (*a*) from $\mathcal{T}^- = H$ to $\mathcal{T}^+ = C$ and (*b*) from $\mathcal{T}^- = C$ to $\mathcal{T}^+ = H$. Upper left, finger movement with the current pattern by $\mathcal{S}(\text{calT}^-, \text{calCP}(t))$, $t < t_t$; upper right, candidates of pattern with the same semi-latus rectum p; lower left, the starting posture of the finger with the new pattern by $\mathcal{S}(\mathcal{T}^+, p)$, $t = t_t$; lower right, finger movement with the new pattern by $\mathcal{S}(\mathcal{T}^+, \mathcal{CP}(t))$, $t > t_t$.

changes, the contact methods described in Sec. 2.3 can also be changed in parallel strategically if needed. Furthermore, it is noted that the notion discussed can be adopted to grasping strategies and object manipulation processes [4,13–20].

5 Conclusions

Extrapolated from real finger posture observed when the human hand grasps a cylindrical object with various cross sections, a numerical framework for joint rotation configuration of a finger has been proposed. The structure of the model consists of a set of systems of nonlinear equations that describe geometric conditions between the phalangers of a finger and the object being grasped. One of conditions to be considered is the shape of object being grasped, each of which is taken from conic sections. Four types of contact methods are taken into consideration in the model development as well. Joint rotation configurations of a finger have been obtained numerically by solving the sets of systems of nonlinear equations for objects with various cross sections by contact methods. Simulation studies and analyses have been conducted regarding the behavior of joint rotation configurations during flexion/extension movements. The simulation results show the possibility of the models to be used in replicating grasping behaviors of the human hand and in robotic/artificial hands design. Future work includes the consideration of objects with cross sections from the curve of order four (quartics) to explore ways of describing various grasping patterns.

Acknowledgment

The authors gratefully acknowledge the support of NSF CAREER award Id # 1751770.

Data Availability Statement

The datasets generated and supporting the findings of this article are obtainable from the corresponding author upon reasonable request. The authors attest that all data for this study are included in the paper. Data provided by a third party listed in Acknowledgment. No data, models, or code were generated or used for this paper.

References

[1] Barbagli, F., Frisoli, A., Salisbury, K., and Bergamasco, M., 2004, "Simulating Human Fingers: a Soft Finger Proxy Model and Algorithm," 12th International Symposium on Haptic Interfaces for Virtual Environment and Teleoperator Systems, Chicago, IL, Mar. 27–28, pp. 9–17.
[2] Kim, B.-H., 2014, "Analysis of Coordinated Motions of Humanoid Robot Fingers Using Interphalangeal Joint Coordination," Int. J. Adv. Rob. Syst., **11**(69), pp. 1–8.
[3] Braido, P., and Zhang, X., 2004, "Quantitative Analysis of Finger Motion Coordination in Hand Manipulative and Gestic Acts," Human Movement Sci., **22**(6), pp. 661–678.
[4] Santello, M., Flanders, M., and Soechting, J. F., 2002, "Patterns of Hand Motion During Grasping and the Influence of Sensory Guidance," J. Neurosci., **22**(4), pp. 1426–1435.
[5] Peña-Pitarch, E., Falguera, N. T., and Yang, J. J., 2014, "Virtual Human Hand: Model and Kinematics," Computer Methods Biomech. Biomed Eng., **17**(5), pp. 568–579.
[6] Miyata, N., Kouchi, M., and Mochimaru, M., 2007, "Generation and Validation of 3D Links for Representative Hand Models," SAE 2007 Digital Human Modeling for Design and Engineering Conference, Seattle, WA, June 12–14, Vol. 1, Paper No. 2007-012512.
[7] Miyata, N., Kouchi, M., Mochimaru, M., Kawachi, L., and Kurihara, T., 2005, "Hand Link Modeling and Motion Generation From Motion Capture Data Based on 3D Joint Kinematics," SAE 2005 Digital Human Modeling for Design and Engineering Conference, Iowa City, IA, June 14–16, Vol. 1, Paper No. 2005-012687.
[8] Savescu, A., Cheze, L., Wang, X., Beurier, G., and Verriest, J., 2004, "A 25 Degrees of Freedom Hand Geometrical Model for Better Hand Attitude Simulation," SAE Digital Human Modeling for Design and Engineering Symposium, Rochester, MI, June 15–17, Vol. 1, Paper No. 2004-01-2196.
[9] Won, J.-S., and Robson, N., 2019, "Control-Oriented Finger Kinematic Model: Geometry-Based Approach," ASME J. Mech. Rob., **11**(6), p. 061007.
[10] McDonald, J., Toro, J., Alkoby, K., Berthiaume, A., Carter, R., Chomwong, P., Christopher, J., Davidson, M. J., Furst, J., Konie, B., Lancaster, G., Roychoudhuri, L., Sedgwick, E., Tomuro, N., and Wolfe, R., 2001, "An Improved Articulated Model of the Human Hand," Visual Computer, **17**(8), pp. 158–166.
[11] Nolker, C., and Ritter, H., 2002, "Visual Recognition of Continuous Hand Postures," IEEE Trans. Neural Netw., **13**(4), pp. 983–994.
[12] Polyanin, A. D., and Manzhirov, A. V., 2007, *Handbook of Mathematics for Engineers and Scientists*, Chapman & Hall/CRC, Boca Raton, FL.
[13] Feix, T., Romero, J., Schmiedmayer, H., Dollar, A. M., and Kragic, D., 2016, "The GRASP Taxonomy of Human Grasp Types," IEEE Trans. Human-Machine Syst., **46**(1), pp. 66–77.
[14] Bowers, D., and Lumia, R., 2003, "Manipulation of Unmodeled Objects Using Intelligent Grasping Schemes," IEEE Trans. Fuzzy Syst., **11**(3), pp. 320–330.
[15] Yu, Y., Li, Y., and Tsujio, S., 2001, "Analysis of Finger Position Regions on Grasped Object With Multifingered Hand," Proceedings of the 2001 IEEE International Symposium on Assembly and Task Planning (ISATP2001), Fukuoka, Japan, May 28–30, pp. 178–183.
[16] Nagashima, T., Seki, H., and Tanako, M., 1997, "Analysis and Simulation of Grasping/Manipulation by Multi-Finger Surface," Mech. Mach. Theory., **32**(2), pp. 175–191.
[17] Bicchi, A., 1995, "On the Closure Properties of Robotic Grasping," Int. J. Rob. Res., **14**(4), pp. 319–334.
[18] Nagai, K., and Yoshikawa, T., 1995, "Grasping and Manipulation by Arm/Multifingered-Hand Mechanisms," Proceedings of IEEE International Conference on Robotics and Automation, Nagoya, Japan, May 21–27, Vol. 1, pp. 1040–1047.
[19] Nagai, K., and Yoshikawa, T., 1993, "Dynamic Manipulation/grasping Control of Multifingered Robot Hands," Proceedings of IEEE International Conference on Robotics and Automation, Atlanta, GA, May 2–6, Vol. 3, pp. 1027–1033.
[20] Cutkosky, M., 1989, "On Grasp Choice, Grasp Models and the Design of Hands for Manufacturing Tasks," IEEE. Trans. Rob. Autom., **5**(3), pp. 269–279.